Natural Resources for Human Health
eISSN: 2583-1194

Original Research

Received 10 July 2026
Revised 15 Aug 2026
Accepted 29 Aug 2026

Natural Resources for Human Health 2026, Vol. 6 (18s): 1170–1192

KEYWORDS:
HSP90, Molecular Chaperone, Cancer, Structure-based drug design, HSP90 isoforms

Structural Insights and Comparative Analysis of HSP90: Implications in Design of Inhibitors

Kanishka Wadhwa[1], Ananya Chandel[1], Amit Kumar[2], Manmeet Kaur[3], Daljeet Masih[4], Sourav Kalra[5]*

[1] University Institute of Pharma Sciences, Chandigarh University, Gharuan, Punjab Email: kanishkawadhwa11@gmail.com
[1] University Institute of Pharma Sciences, Chandigarh University, Mohali, Punjab, India Email: ananyachandel@gmail.com
[2] Department of Entomology, Punjab Agricultural University, Ludhiana, Punjab, India Email: Ak.bhardwaj567@gmail.com
[3] Department of Pharmaceutical Chemistry, Khalsa College of Pharmacy, Amritsar, Punjab, India Email: kaurmanmeet639@gmail.com
[4] Golden College of Pharmacy, Gurdaspur, Punjab, India Email: Kiranjotgill@yahoo.co.in
[5] Sardar Beant Singh State University, Pathankot Road, Gurdaspur, Punjab Email: nonakalra@gmail.com
Corresponding author: Dr. Sourav Kalra, nonakalra@gmail.com

ABSTRACT: Heat shock protein 90 (HSP90) is an important molecular chaperone involved in the stabilization and regulation of multiple client proteins that contribute to cancer cell growth, survival, and progression. Its central role in oncogenic signaling has made HSP90 an attractive target for anticancer drug development. However, despite extensive efforts to develop potent HSP90 inhibitors, clinical translation has remained challenging, highlighting the need for a more comprehensive understanding of the structural and mechanistic determinants of HSP90 inhibition. This review provides a structural and mechanistic analysis of HSP90, with particular emphasis on the domain organization, ATP-dependent chaperone cycle, conformational dynamics, and structural differences between HSP90α and HSP90β. The binding characteristics of HSP90 inhibitors are discussed according to their interaction with the N-terminal ATP-binding region, C-terminal region, and alternative or allosteric binding sites, with emphasis on the distinction between conserved interactions and structural features that may support isoform or paralog selectivity. Recent computational approaches, including virtual screening, molecular docking, and molecular dynamics simulations, are critically evaluated in relation to experimental biochemical, cellular, and structural validation. The review further examines the clinical development of selected HSP90 inhibitors and identifies factors contributing to limited clinical translation, including toxicity, adaptive heat-shock responses, pharmacokinetic and pharmacodynamic limitations, and difficulties in achieving adequate selectivity and therapeutic efficacy. Collectively, these findings indicate that high binding affinity within the conserved N-terminal ATP-binding pocket alone may be insufficient for successful therapeutic development. Future HSP90 inhibitor design should therefore integrate structural selectivity, conformational dynamics, adjacent sub pockets, alternative binding sites, target engagement, and appropriate experimental validation to support the development of more selective and clinically useful HSP90-targeted therapies.

Natural Resources for Human Health
eISSN: 2583-1194

1. INTRODUCTION

The heat shock response was first discovered in 1962 by Italian geneticist Ferruccio Ritossa while studying the fruit fly, Drosophila[1]. Over time, researchers found that heat shock proteins, or HSPs, are highly conserved through evolution and are present in nearly all living organisms, from bacteria to humans[2]. Even under normal conditions, HSPs make up about 5-10% of all cellular proteins and are continuously expressed [3]. They perform a wide range of essential functions, including transporting proteins within the cytosol, endoplasmic reticulum, and mitochondria, repairing damaged proteins, and helping fold or refold misfolded proteins[4]. HSPs can be broadly classified into five major categories: the small HSP family, HSP60, HSP70, HSP90 and large HSP family depending on their molecular size, as shown in Fig. **1** and Table **1** [5].

HSP90 is an important molecular chaperone that contributes to cellular homeostasis and survival under stressful conditions **Fig. 2** [6]. Among the heat shock proteins, HSP90 is prominent because of its involvement in various physiological cellular processes and progression in various disease[7]. HSP90 regulates several important processes within cells such as their folding and breakdown of proteins, cell signaling, cell growth, survival and programmed cell death by acting with co-chaperones and client proteins [8].

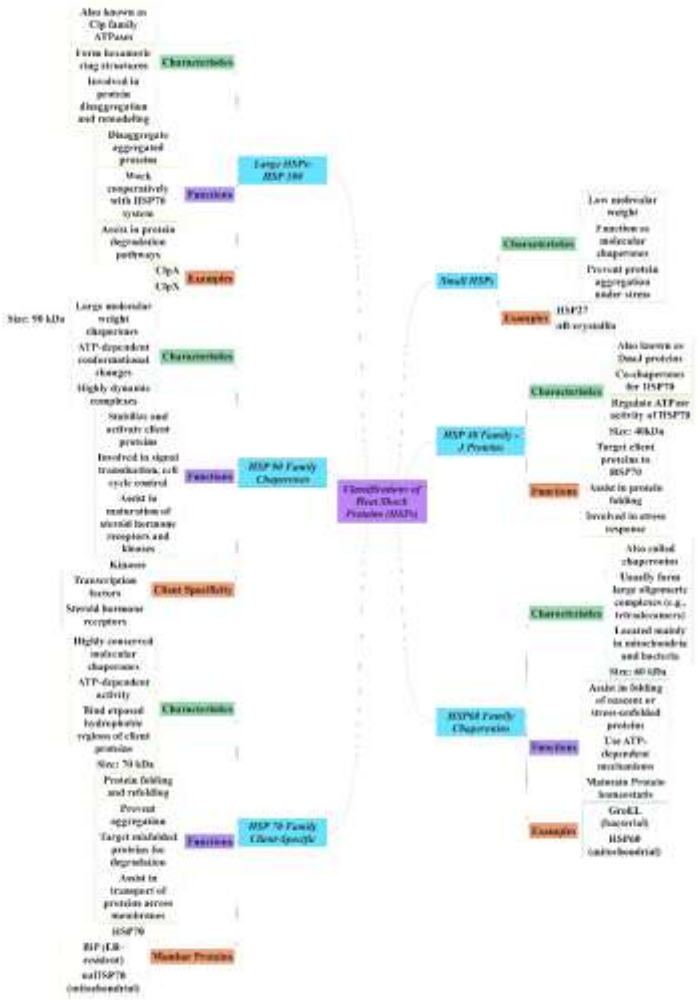


Fig. 1. Classification of Heat Shock Proteins (HSPs)

Natural Resources for Human Health
eISSN: 2583-1194

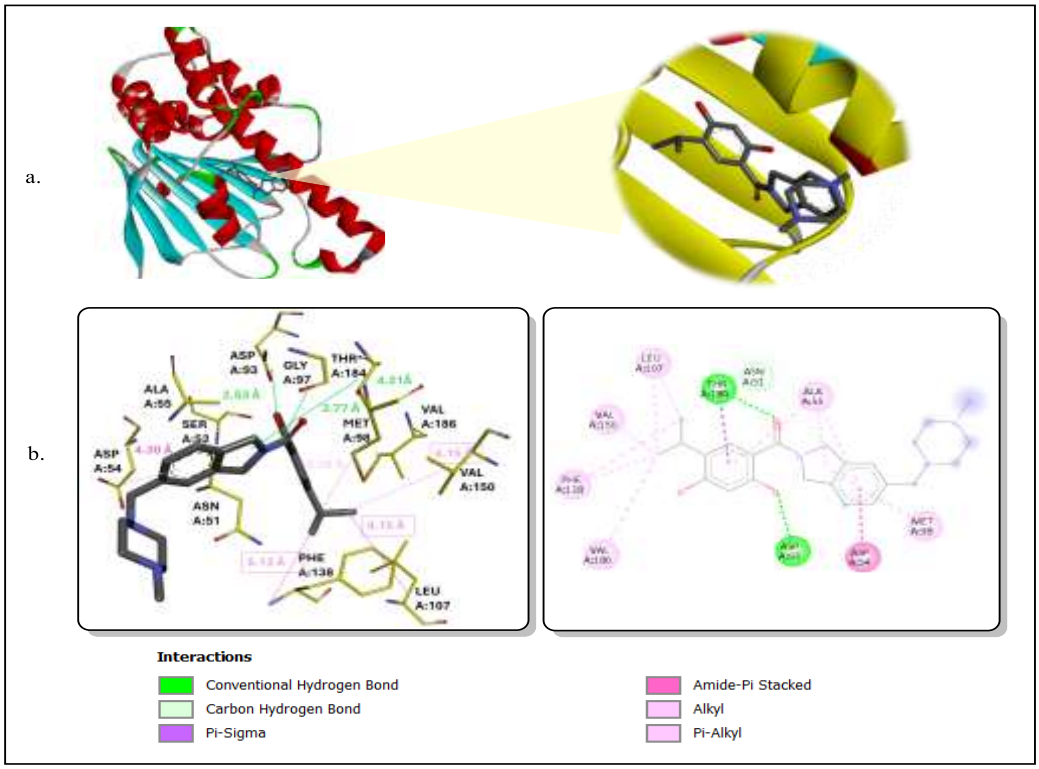


Fig. 2. (a) The crystal structure of the HSP90 protein corresponding to PDB ID 2XJX defines its tertiary structure. **(b)** Three-dimensional visualization emphasizes the topology of the binding cavity and the extent to which the various key residues are spatially organized to play an important role in mediating molecular recognition. The accompanying two-dimensional interaction profile provides a complete description of the interaction network, which explains the underlying mechanisms of the stabilization and specificity of ligand binding.

Table 1: Key Family of Human Heat Shock Proteins: Sizes, Genes, Functions and Cellular Roles.

HSP Family	Approximate Size (kDa)	Related Human Genes	Location	Main Roles and Actions	Reference
HSP10	About 10 kDa	GroES	Mitochondria	Acts as a helper molecule supporting HSP60 with protein folding inside mitochondria	[9]
HSP27	20-30 kDa	HSPB1	Cytoplasm nucleus	Protects cells by preventing protein clumping and supports the cell's structural work	[9]
HSP32	Approximately 32 kDa	HSP32(HO-1)	Cytoplasm and endoplasmic reticulum	Breaks down heme molecules, playing a role in the response to oxidative stress	[10]
HSP40	35-54 kDa	DNAJ family	Cytoplasm and nucleus	Works alongside HSP70 to regulate	[11]

				protein folding and repair	
HSP60	Between 55-64 kDa	Cpn60	Mitochondria	Helps newly arrived proteins fold correctly inside mitochondria	[12]
HSP70	65-80 kDa	HSPA family	Cytoplasm, ER, mitochondria	Major chaperone facilitating protein folding and transport, preventing harmful aggregates	[13]
HSP90	About 81-99 kDa	HSPC family	Cytoplasm, mitochondria, and nucleus	Stabilises and activates many key proteins involved in cell signaling and growth	[6]
HSP100	100 kDa and above	HSP100	Cytoplasm and mitochondria	Disassembles protein aggregates, assisting in protein recovery	[14]
HSP110	More than 100 kDa	HSPH family	Cytoplasm and nucleus	Supports HSP70 by exchanging nucleotides, enhancing protein folding.	[15]

In this review, we focus on the structural and mechanistic features of HSP90 that are relevant to inhibitor recognition and anticancer drug development, with emphasis on HSP90α/β differences, conformational dynamics, ligand binding, and alternative binding sites. Computational approaches and their experimental validation are also critically discussed, along with the challenges of clinical translation and future strategies for developing selective HSP90 inhibitors.

2. HSP90: A Master Regulator in Progression of Cancer

Heat shock protein 90 (HSP90) is an important molecular chaperone that has been thoroughly studied in cancer research because it plays a vital role in tumor growth and progression [16]. In cancer cells, HSP90 helps to fold, stabilize and activate different client proteins. Many of these proteins are oncogenic drivers which are critical for the development and maintenance of tumors [17]. This chaperone functions through ATP-dependent conformational changes, interacting with the client molecule such as kinase, steroid hormone receptor and transcription factors [18]. These include HER2, AKT and mutated p53. It prevents the degradation of these proteins and enhances their functions in battling cancer [19]. HSP90 also aids cancer cells to cope with various stresses inside the cell, such as oxygen deprivation and protein damage [20]. This support helps to guide survival and adaptability of tumors [21]. Structurally, HSP90 has three major parts. The N-terminal domain consists of ATP and client binding sites. The middle domain is known to be responsible for ATP hydrolysis. The C-terminal domain is important for dimerisation and interaction. The ATPase activity drives the chaperone cycle, which is essential for the maturation of client [22]. The overexpression of HSP90 is associated with aggressive disease and poor prognosis in many cancers. Because of this HSP90 is a major target for cancer treatments [21]. Inhibitors such as geldanamycin, 17-AAG and ganetespib attempt to inhibit its ATPase activity. This action causes the degradation of client proteins and death of tumor cells. Clinical trials have demonstrated that HSP90 inhibitors have the ability to target several cancer-related pathways simultaneously [7]. Furthermore, an active HSF1-mediated heat shock response with increased HSP expression is observed in cancer cells [23]. This response makes one more resistant to therapy and improves survival. HSP90 Inhibitors Can Interfere With This Process Revealing Complicated Treatment Possibilities [24].

2.1 Isoforms of HSP90 and their significant role in cancer

Human cells contain many isoforms of HSP90, each with distinct cellular locations and biological functions, rather than a single protein [25]. HSP90α, HSP90β, GRP94 and TRAP1 are the primary human HSP90 isoforms that are found in cytosol, endoplasmic, and mitochondria, among other cellular compartments [26]. Because of their significant roles in numerous physiological processes, the cytosolic isoforms HSP90α and HSP90β are the most prevalent among them and have been thoroughly researched. The human HSP90AB1 gene produces the HSP90β isoform, whereas the HSP90AA1 gene encodes the HSP90α isoform. These two proteins most likely developed comparable but somewhat specialized roles within the cell because of gene duplication during evolution [27].

HSP90α and HSP90β have around 84-85% sequence identity, indicating their high structural conservation while performing related roles [28]. Both isoforms function as ATP-dependent homodimers, which means that two identical protein units come together to create the functional chaperone complex [29]. HSP90β is typically regarded as a constitutively expressed regarded as a constitutively expressed protein, which means that it is constantly produced in cells and aids in regular cellular maintenance [29]. On the other hand, HSP90α is referred to as a stress-inducible isoform, and when cells encounter stress conditions as heat shock, oxidative stress, or tissue injury, its expression dramatically rises [30]. These variations show that while HSP90α is crucial for assisting cells in adjusting to stressful situations, HSP90β mostly maintains regular cellular processes [31]. HSP90α has also been connected to cancer metastasis and progression since it can be produced outside the cell in some tumor types. After the release into the extracellular environment, HSP90α can activate matrix metalloproteinases such as MMp-2, which break down components of the extracellular matrix and encourage cancer cell invasion [32]. Extracellular HSp90's role in wound healing, cell migration, and inflammatory responses can be exploited by cancer cells to boost metastasis [33]. On the other hand, as HSP90β mainly supports basic cellular survival and protein stability, it is essential for appropriate cell viability [20]. Because HSP90 can stabilize many oncogenic proteins simultaneously, it has attracted a lot of attention as a possible target for the development of anticancer medicines [17]. Consequently, several HSP90 inhibitors have been created to disrupt the chaperone cycle, which leads to the degradation of several client proteins associated with cancer [34]. However, because inhibitors that block all HSP90 isoforms frequently have undesirable side effects, the development of isoform-specific inhibitors that solely target HSP90α or HSP90β has increased [30]. The role of HSP90 in cancer focuses on its ATP-dependent chaperone function. This function stabilizes a wide range of cancer-causing proteins and helps cancer cells survive in stressful conditions [35]. There are some different protein PDB ID's for HSP90, HSP90α, and HSP90β which are mentioned in Table **2.**

Table 2: Different PDB IDs of HSP90, HSP90α, and HSP90β with their Resolution, Ligand structure, Amino acid interactions, and PDB Ligand.

PDB ID	Species	Isoform / Protein	Construct / Domain	Ligand	Resolution (Å)	Binding site / Structural state	Key structural significance
7RY1 [36]	*Homo sapiens*	HSP90α	Middle + C-terminal (MC) domains	MDCC	3.52	Allosteric MC-domain pocket	Reveals a hydrophobic allosteric pocket at the MC-domain interface; ligand binding is associated with loop stabilization, conformational changes, and HSP90α oligomerization.

8AGI [37]	*Homo sapiens*	HSP90α	N-terminal domain (NTD)	JMC31	2.10	N-terminal ATP-binding pocket	Provides a high-resolution structure of a 1,2,3-triazole-based inhibitor bound to the HSP90α NTD, supporting structure-guided analysis of the ATP-binding site.
8SBT [38]	*Homo sapiens*	HSP90α	N-terminal domain (NTD)	PU-H36	1.50	N-terminal ATP-binding pocket	High-resolution purine-inhibitor complex illustrating ligand accommodation within the conserved N-terminal pocket.
7HB2 [39]	*Homo sapiens*	HSP90α	N-terminal domain (HSP90N)	FL0184	1.67	N-terminal ligand-binding site	Fragment-bound structure providing structural information for fragment-based exploration of the HSP90α N-terminal pocket.
7H9U [40]	*Homo sapiens*	HSP90α	N-terminal domain (HSP90N)	Fr12864	1.94	N-terminal ligand-binding site	Fragment-screening structure that provides an additional experimentally observed ligand-binding mode in the HSP90α N-terminal region.
7D24 [41]	*Mus musculus*	HSP90α	N-terminal domain	GQ3 (compound 4b)	1.55	N-terminal ATP-binding/hydrophobic pocket	Demonstrates binding of a purine-based inhibitor within the ATP-binding pocket and provides structural information on

							the adjacent hydrophobic region.
7D25 [41]	*Mus musculus*	HSP90α	N-terminal domain	GQ6 (compound 14)	1.65	N-terminal ATP-binding/hydrophobic pocket	Shows an alternative purine-based inhibitor bound in the N-terminal pocket; the ligand adopts an L-shaped binding arrangement involving the ATP-binding and hydrophobic regions.
6GPR [80]	*Homo sapiens*	HSP90α	N-terminal domain	cAMP	2.35	Nucleotide-binding site	Represents a nucleotide-associated HSP90α N-terminal state and provides a structural reference for nucleotide recognition rather than conventional inhibitor binding.
6GPT [42]	*Homo sapiens*	HSP90α	N-terminal domain	AMPCP	2.00	Nucleotide-binding site	Provides an ATP-analogue-associated structural state useful for understanding the N-terminal nucleotide-binding environment
6GQR [42]	*Homo sapiens*	HSP90α	N-terminal domain	AMPCPP	2.05	Nucleotide-binding site	Provides another ATP-analogue-bound state for comparison of nucleotide-associated conformations

							of the HSP90α N-terminal domain.
3NMQ [43]	*Homo sapiens*	HSP90β	N-terminal domain	EC144	2.20	N-terminal ATP-binding pocket	Demonstrates inhibitor recognition by the HSP90β N-terminal domain and provides a structural reference for β-isoform ligand binding.
5UC4 [44]	*Homo sapiens*	HSP90β	N-terminal domain	83S	2.05	N-terminal ATP-binding pocket	Structure-guided HSP90β-selective inhibitor complex; useful for examining features associated with β-isoform-directed ligand design.
5UCH [44]	*Homo sapiens*	HSP90β	N-terminal domain	871	2.65	N-terminal ATP-binding pocket	Provides another HSP90β inhibitor-bound structure for comparison of ligand accommodation within the N-terminal pocket.
5UCI [44]	*Homo sapiens*	HSP90β	N-terminal domain	874	2.70	N-terminal ATP-binding pocket	Shows an alternative inhibitor scaffold within the HSP90β N-terminal pocket and contributes to structure-guided isoform-selective inhibitor design.
5UCJ [44]	*Homo sapiens*	HSP90β	N-terminal domain	KU3	1.69	N-terminal ATP-binding pocket	High-resolution HSP90β–KU3 complex

							providing structural information for inhibitor recognition and β-isoform-selective design.
6N8Y [45]	*Homo sapiens*	HSP90β	N-terminal domain	PU-11-trans	1.55	N-terminal ATP-binding pocket	Together with corresponding HSP90α structures, provides direct structural evidence for differences in the ATP-binding pocket that can be exploited for α/β selectivity.
7K9S [40]	*Cryptococcus neoformans*	Fungal Hsp90	Nucleotide-binding domain	NVP-AUY922	3.21	N-terminal nucleotide-binding pocket	Fungal Hsp90 structure illustrating species-dependent ligand recognition and ligand-induced conformational behaviour; should not be directly equated with human HSP90 structures.
7K9U [40]	*Cryptococcus neoformans*	Fungal Hsp90	Nucleotide-binding domain	BUCMD 00429	1.92	N-terminal nucleotide-binding pocket	High-resolution fungal Hsp90 complex illustrating ligand-induced structural rearrangements relevant to fungal-versus-human selectivity.
7K9W [40]	*Cryptococcus neoformans*	Fungal Hsp90	Nucleotide-binding domain	BUCMD 00461	2.13	N-terminal nucleotide-binding pocket	Provides another fungal Hsp90 ligand-bound conformation

							and supports comparison of species-dependent pocket flexibility and ligand accommodation.

2.2 Structural organization of HSP90

The structural arrangement of HSP90 has a significant impact on its ligand-binding properties and provides several therapeutic intervention options[46]. HSP90 undergoes substantial conformational changes during its ATP-dependent chaperone cycle, indicating that in addition to static residue interactions, pocket shape, flexibility, and the proteins structural state all affect ligand binding[29]. HSP90 is a dynamic molecular chaperone that generally functions as a homodimer. Each HSP90 monomer is organized into three functionally distinct but closely interconnected regions, such as the N-terminal domain (NTD), middle domain (MD), and C-terminal domain (CTD)[46]. In the cytosolic HSP90 isoforms, the NTD and MD are separated by the flexible, charged linker that allows movement between the domains. Rather than functioning as independent units, these domains communicate with one another throughout the HSP90 chaperone cycle, which allows the changes at one region of the protein to influence the structural and functional behavior of the other[47].

The MD is positioned between the NTD and CTD and plays an important role in client–protein recognition as well as regulation of ATP hydrolysis. The MD contains a conserved catalytic loop that contributes to the ATPase cycle by interacting with the γ-phosphate of ATP bound within the NTD. In the yeast HSP0 (Hsp 82), Arg380 within this loop interacts with the γ-phosphate and helps stabilize the NTD-MD interaction required for formation of the closed, ATPase–competent conformation[48].

CTD plays a role in keeping HSP90 in a dimerized state. It gives spots for co-chaperones and regulatory proteins to bind [46]. Cytosolic HSP90 proteins also carry a MEEVD motif at their far-right end. This short sequence is recognized by TPR-containing co-chaperones and helps bring regulatory parts into the HSP90 complex. These connections help pick which client proteins will be handled and shape how the chaperone cycle moves forward [49].

In general, the three parts of HSP90 work together as one functional whole. ATP. ATP hydrolysis at the NTD drives shape changes that involve MD and CTD. As a result, HSP90 can switch between shapes while it matures client proteins. This deep communication between the domains is also important for drug discovery. It offers chances to affect HSP90 by targeting not only the stable N-terminal ATP pocket but also other regulatory and allosteric sites [50].

2.3 Conformational Dynamics and Structural States of HSP90

HSP90 is not a rigid molecular machine, but its chaperone function is driven by the continuous sampling of different conformational states. The two protomers of the HSP90 dimer move in a coordinated manner in response to nucleotide binding, hydrolysis, client association, and interaction with co-chaperones. These structural transitions enable HSP90 to adopt a conformation as a function of the phase of the chaperone cycle[50].

Instead of acting as a structurally static target, the domains of HSP90 migrate together during the chaperone cycle[50]. As a result, only one conformational state may be represented by a single empirically determined structure and not all ligand-accessible binding possibilities may be captured[51]. Because of this using conformational flexibility in the hunt for inhibitors may uncover distinct binding mechanisms or fleeting areas that are concealed by static structures[52]. By analysing pocket stability, ligand interactions, and conformational changes over time, molecular dynamics simulations can aid structural and docking research however rather than being concrete proof of biological activity, computationally predicted conformation should be regarded as hypothesis that require biochemical or experimental validation[53].

2.4 Structural opportunities Beyond the Conserved N-Terminal ATP-Binding Pocket

Since the conserved N-terminal ATP-binding pocket offers a precise location for ligand recognition, it has been the focus of HSP90 inhibitor research[54]. However, specific inhibition is very challenging to do because of the strong conservation of this region among HSP90 isoforms[55].

Consequently, there may be greater potential to enhance treatment efficacy and selectivity through structural techniques that consider nearby sub pockets, transient conformational states, and unique binding areas. Structure-guided optimisation can take advantage of differences in residue composition, pocket geometry, or flexibility seen in sub pockets around the canonical ATP- binding site[56].

In a similar vein, may become accessible or adopt favourable geometries during specific stages of the HSP90 chaperone cycle. Without directly affecting ATP binding, HSP90 function can also be changed via allosteric or C-terminal regions. When considered collectively, these structural choices shift the emphasis of inhibitor creation from optimising interactions within a conserved pocket to utilising protein dynamics, alternative regulatory sites, and local structural differences[57].

2.5 Structural diversity and functional specialization of HSP90 paralogs

Members of the HSP90 family share a conserved three-domain organization and related chaperone functions but are not functionally interchangeable. The major HSP90 paralogs in humans are cytosolic HSP90α and HSP90β, endoplasmic-reticulum resident GRP94, and mitochondrial paralog TRAP1. Their common structural framework is therefore accompanied by differences in sequence, subcellular localization, conformational behaviour, client preference, and regulatory interactions, which allow each paralog to operate within a distinct cellular environment[58].

The most closely related family members are the cytosolic isoforms HSP90α and HSP90β, which share ~85% overall sequence identity. HSP90β is usually constitutively expressed, whereas HSP90α is more strongly induced by cellular stress and often associated with stress-adaptive and tumor-related processes[59].The two proteins are highly similar but not completely redundant. Their biological activities can be influenced by differences in their sequence, post-translational regulation, interaction partners, and client preferences[60]. These differences are particularly relevant to drug discovery, as the N-terminal ATP-binding pockets of HSP90α and HSP90β are very similar, making it much more difficult to design selective ligands than to distinguish between the cytosolic proteins and GRP94 or TRAP1[61]

These paralogs also vary in their co-chaperone networks and client repertoires. Cytosolic HSP90α and HSP90β interact with a rather large set of co-chaperones, including HOP, p23, Aha1, and Cdc37, that control client transfer, conformational switching, and ATPase regulation[50]. By contrast, GRP94 interacts with a smaller group of ER-associated regulatory proteins, and TRAP1 functions in the mitochondrial environment with a different regulatory network[58].

2.6 Difference between HSP90α & HSP90β

A crucial molecular chaperone, heat shock protein 90 controls the folding, stability, and activity of many signaling proteins involved in cellular homeostasis and the development of cancer [62]. Human cells have several isoforms of HSP90; the two main cytosolic forms, HSP90α & HSP90β [25].- Functionally, Hsp90α is often associated with cell migration, wound healing, and tumor formation, particularly when it is released into the extracellular environment [63]. Extracellular Hsp90α has been shown to promote tumor invasion and metastasis by facilitating the activation of signaling pathways that activation of signaling pathways that regulate cell motility and matrix remodeling [64]. However, HSP90β functions as a housekeeping molecular chaperone under normal physiological conditions, mainly supporting signal transmission, protein folding, and cell survival [28]. Because many carcinogenic proteins depend on HSP90 for stability, both indirectly contribute to tumor growth, survival, and therapy resistance **Fig. 3** [65]

Natural Resources for Human Health
eISSN: 2583-1194

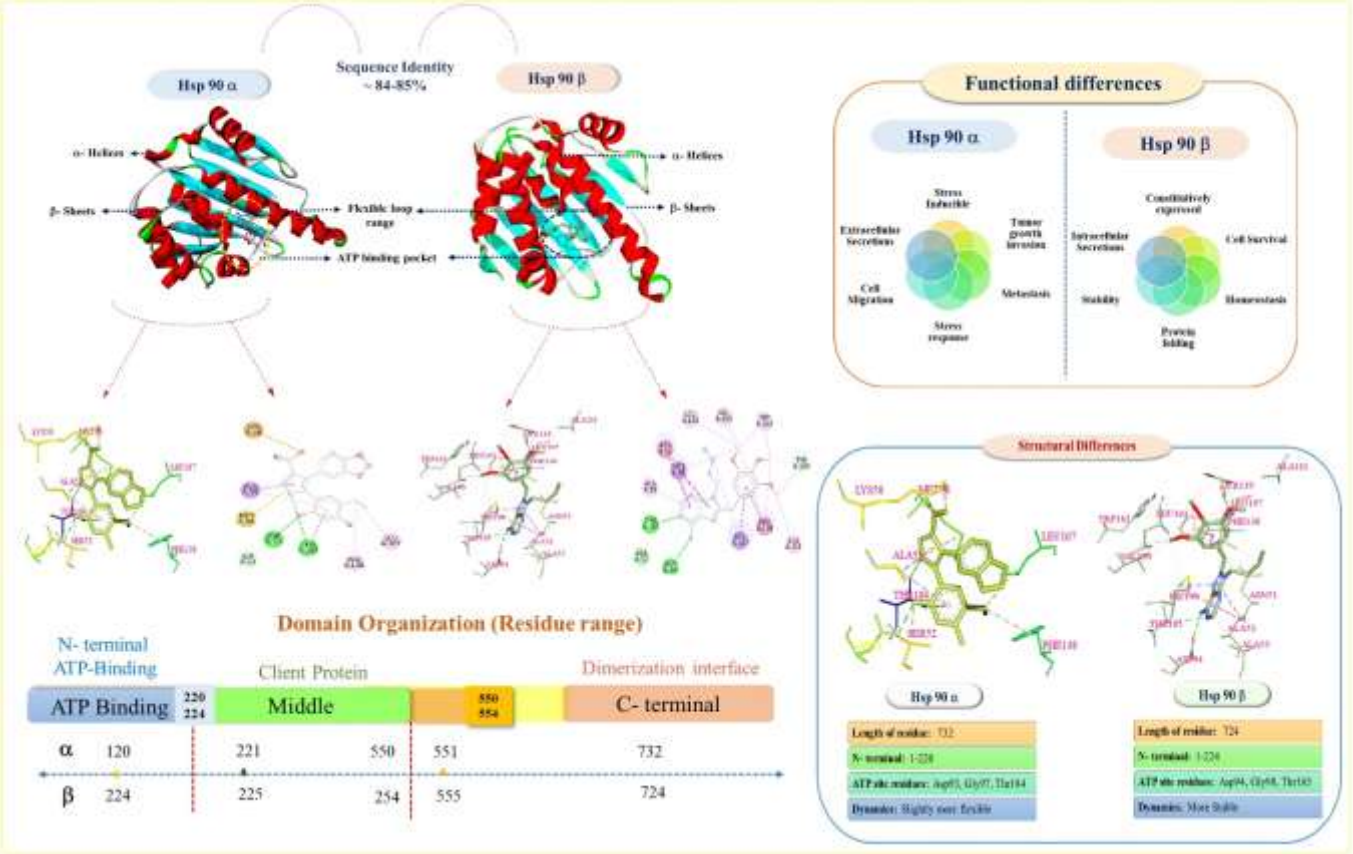


Fig. 3. Structural comparison of the N-terminal domains of HSP90α and HSP90β. Ribbon representation of the N-terminal ATP-binding domains of human HSP90α (PDB ID:1YC3) and HSP90β (PDB ID: 1UYM) are shown. The ATP-binding pocket is located within the central cavity of the N-terminal domain. Despite belonging to different isoforms, the high structural conservation of this domain explains the similar binding modes of Hsp90 inhibitors in both proteins.

Table 3 Structural and Functional comparison of HSP90α and HSP90β

Feature	HSP90α	HSP90β	Relevance to inhibitor design
Gene	HSP90AA1	HSP90AB1	Different genetic origin
Sequence identity	~85% with HSP90β	~85% with HSP90α	Non-identical residues may support selectivity
Expression	Stress inducible	Constitutive	Different therapeutic rationale
Major functions	Stress response, migration, tumor progression	Proteostasis, survival, cellular maintenance	May enable disease/isoform-specific targeting
ATP-binding pocket	Highly conserved	Highly conserved	Conserved region supports potency
Residue numbering	Isoform/construct dependent	Isoform/construct dependent	Equivalent residues must be mapped before comparison
Pocket differences	Local differences around conserved pocket	Local differences around conserved pocket	Can be exploited for selectivity
Conformational	Dynamic ATPase cycle	Dynamic ATPase cycle	Flexible/sub pocket regions may

dynamics			provide selectivity
Drug-design strategy	Target non-conserved residues/sub pockets	Target non-conserved residues/sub pockets	Development of isoform-selective inhibitors

Although HSp90α and HSP90β share a highly conserved overall design and ATP-binding function, structural differences between them may have a substantial impact on inhibitor selectivity[44]. As a result, it is critical to distinguish between traits shared by the two isoforms and variations in sequence, residue numbering, pocket differences, and conformational dynamics[66]. Only interactions with highly conserved residues within the N-terminal ATP-binding pocket are unlikely to yield strong isoform selectivity[45]. Instead, differences in nearby sub pockets, pocket geometry, flexibility, and surrounding residues may present opportunities for the creation of isoform-selective inhibitors. To determine if these differences impact conformational preferences, interaction patterns, or ligand-accessible space, a comparison between HSP90α and HSP90β should go beyond simply identifying sequence variants[56].

Importantly, the presence of a sequence variation does not always indicate an isoform-selective interaction. The location of a residue in respect to the ligand-binding site, its effect on pocket geometry or flexibility, and any corroborating structural or biochemical information all influence its impact. Therefore, a combination of structural, computational, and experimental information should be used to evaluate suspected HSP90α/β selectivity rather than relying on residue level changes[45].

3. Inhibitors of HSP90 Reported in The Past Few Years

HSP90 has emerged as an important therapeutic target in cancer because it maintains the stability and function of multiple client proteins involved in tumor growth, survival, and signaling [20]. HSP90 inhibitors have been developed against different structural regions of the chaperone, particularly the N-terminal ATP-binding domain, C-terminal region, and isoform-specific sites [28]. Rather than classifying these inhibitors solely according to chemical structure, their therapeutic properties can be discussed in relation to their binding site, mechanism of action, isoform selectivity, and ability to overcome limitations associated with HSP90 inhibition[67].

3.1 N-Terminal HSP90 Inhibitors: By interacting with the ATP-binding pocket in the N-terminal domain of HSP90, N-terminal inhibitors stop ATP hydrolysis, which is required for the chaperone cycle [68]. ATP binding and hydrolysis are necessary for conformational changes in HSP90 that allow proper folding and stabilization of client proteins [29]. When N-terminal inhibitors bind to this ATP pocket, they prevent the formation of active HSP90 complexes and promote client protein degradation through the proteasome route [69]. This family of HSP90 is the largest and most extensively studied in the hunt for anticancer medications [70]. However, a significant obstacle to the development of selective inhibitors is the high degree of conservation of the N-terminal ATP-binding region among HSP90 isoforms and paralogs. Strong ligand binding and increased inhibitory potency can result from interactions with highly conserved residues, but they might not be enough to differentiate HSP90α from HSP90β or the other HSP90 paralogs. Therefore, enhanced isoform selectivity does not always follow from increased ligand interactions inside the conserved ATP-binding-region[71].

Clinical translation is similarly affected by this structural conservation. Widespread suppression of some HSP90 paralogs may cause dose-limiting toxicity and disrupt regular chaperone functioning. Furthermore, N-terminal inhibition may lessen the long-term therapeutic efficacy of treatment by triggering the compensatory heat-shock response, which includes increased production of cytoprotective chaperones such HSP70[72].

One of the first drugs discovered to suppress HSP90 activity was Geldanamycin, one of several early inhibitors derived from natural materials. More stable substances like 17-AAG (tanespimycin) and 17-DMAG (alvespimycin) were created for clinical use because of geldanamycin's toxicity [73]. Some N-terminal inhibitors have demonstrated drawbacks such as toxicity and heat-shock response activation despite their encouraging anticancer potential, which may lessen therapeutic efficacy [7].

3.2 C-Terminal HSP90 Inhibitors: C-terminal inhibitors interact with the C-terminal domain of HSP90, which is responsible for dimerisation and interactions with co-chaperone proteins. Because they reduce HSP90 activity without significantly causing the heat shock reaction, these compounds are attractive alternatives to N-terminal inhibitors [18]. One of the first C-terminal inhibitors identified was novobiocin, a coumarin antibiotic that attaches to the C-terminal nucleotide-binding site of HSP90. Numerous analogues with improved anticancer effectiveness have been created by the structural modifications of novobiocin

[74]. Developing novel C-terminal inhibitors that can disrupt co-chaperone interactions or stop HSP90 dimerisation has been the aim of contemporary medicinal chemistry [75].

3.3 Isoform-Selective HSP90 Inhibitors: Each of the HSP90 protein family's isoforms, including GRP94, TRAP1, HSP90α, and HSP90β has a distinct biological function [76]. All the isoforms are usually targeted simultaneously by conventional HSP90inhibitors, which may cause toxicity and other issues [22]. Isoform-selective inhibitors have the potential to preserve the efficacy of therapy but minimize the side effects of general HSP90 inhibition [77]. One example is pimitespib, a clinically approved HSP90 inhibitor used in Japan to treat gastrointestinal stromal tumors. In addition, recent work has focused on the development of selective inhibitors that target some isoforms, such as HSP90β, which could improve therapeutic results in cancer treatment l [78].

3.4. Evolution of HSP90 Inhibitors: The development of HSP90 inhibitors was initiated by the discovery of natural products that interfere with the ATP-dependent activity of the chaperone. The finding that geldanamycin binds to the N-terminal ATP-binding pocket of HSP90 was an important proof of concept that pharmacological inhibition of HSP90 can destabilize and/or prevent maturation of multiple oncogenic client proteins [79]. Although the activity of geldanamycin was not suitable for clinical development due to toxicity and poor pharmacological properties, this led to the creation of more stable derivatives, including 17-AAG (tanespimycin) and 17-DMAG (alvespimycin) [80]. These compounds proved that inhibition of HSP90 could simultaneously impact multiple signaling pathways involved in tumor growth, survival, angiogenesis, and metastatic progression, prompting extensive investigation of HSP90 as a therapeutic target[81]. After drug-development efforts, several synthetic N-terminal HSP90 inhibitors with improved physicochemical and pharmacological properties were developed. Compounds such as AUY922, ganetespib, BIIB021 and other resorcinol and purine-based inhibitors went into preclinical and clinical studies, demonstrating the ongoing interest in targeting the conserved ATP-binding site[82]. A major turning point was the identification of geldanamycin, a benzoquinone ansamycin antibiotic, which was then shown to interact with the N-terminal nucleotide-binding site of HSP90. Structural and biochemical studies showed that geldanamycin binds to the ATP-binding pocket and blocks the normal nucleotide-dependent progression of the HSP90 chaperone cycle[83].

Although geldanamycin provided convincing proof of principle, its unfavourable pharmacological properties and toxicity precluded its development as a practical therapeutic agent. These limitations prompted the synthesis of derivatives with improved stability and drug-like properties. One of the most studied derivatives was 17-allylamino-17-demethoxygeldanamycin (17-AAG; tanespimycin), which was taken into clinical development and constitutes an important milestone in the translation of HSP90 inhibition from experimental systems to humans[84]. 17-DMAG (alvespimycin), a second-generation derivative, was developed with the aim of improving aqueous solubility and pharmacokinetic behaviour[85]. The clinical status and development outcomes of selected HSP90 inhibitors are summarized in Table 4 and Fig 4.

Table 4. Clinical Development Status and Outcomes of Selected HSP90 Inhibitors

HSP90 inhibitor	**Clinical stage/status**	**Status**	**Key reason/outcome**
Pimitespib	Phase III	**Approved in Japan**	Positive Phase III development in GIST
Luminespib	Phase II	**Discontinued**	Clinical development discontinued
BIIB021	Phase I	**Discontinued**	Clinical development discontinued
Ganetespib	Phase III	**Discontinued**	Phase III development did not demonstrate the required clinical benefit
HSP990	Phase I	**Terminated**	Clinical development discontinued
PU-H71	Phase I	**Clinical evaluation**	No regulatory approval
Onalespib	Phase II	**Development discontinued**	Clinical development discontinued
17-DMAG	Phase I/II	**Discontinued**	Toxicity concerns

Natural Resources for Human Health
eISSN: 2583-1194

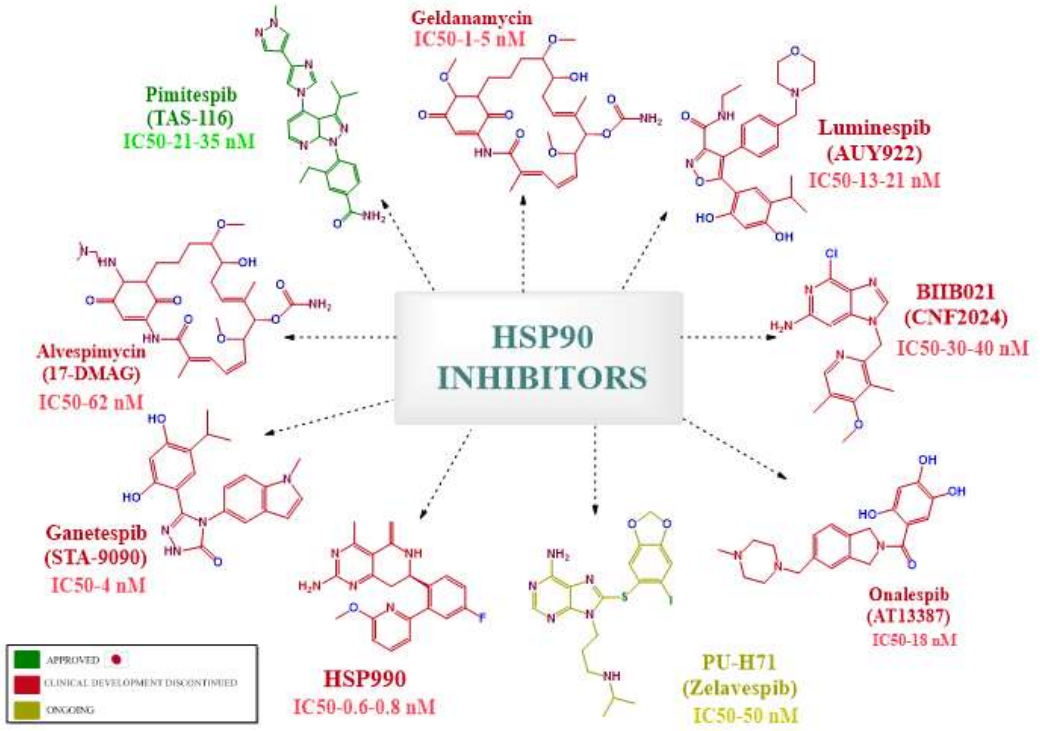


Fig. 4. Inhibitors of HSP90 classified according to clinical status. Chemical structures are represented with corresponding IC_{50} values, in which colour denotes clinical progression.

Strong target binding and encouraging preclinical activity do not always translate into effective anticancer therapy, as demonstrated by the clinical development of HSP90 inhibitors. Several inhibitors have started clinical trials, but their development has been hampered by pharmacological restrictions, adaptive cellular responses, toxicity, limited therapeutic benefit, and challenges in identifying patient populations who are responsive. These results imply that increasing affinity for the highly conserved N-terminal ATP-binding pocket by itself could not offer sufficient therapeutic window or selectivity. Future HSP90 inhibitor design should therefore consider binding affinity in addition to isoform or paralog selectivity, pharmacokinetic characteristics, target engagement, cellular reactions, and tumor-specific reliance on HSP90 client proteins. Pimitespib, which has been approved in Japan for advanced or resistant gastrointestinal stromal tumors, serves as an example of the promise of paralog-selective targeting.

4. COMPUTATIONAL APPROACHES FROM RECENT LITERATURE

Aboalroub *et al.*, 2025 has employed the method of virtual screening to identify a novel compound belonging to the isoxazole family as an inhibitor of heat shock protein 90 (HSP90), which plays an important role in cancer progression. They screened the ZINC database to find molecules similar in structure to the HSP90 inhibitor Luminespib. Molecular docking analysis showed that Compound 1 had better binding affinities to the ATP-binding site of HSP90 than Luminespib. These compounds interacted with important amino acid residues such as Gly97, Asn51 and Lys58 by hydrogen bonds and hydrophobic contacts. Additionally, some candidates-built salt bridges with acidic residues on HSP90, making their binding more stable. The in-silico prediction of toxicity revealed that a number of these compounds are like or even more effective than Luminespib against various cancer cell lines. These studies paved the way for further optimization through medicinal chemistry studies and experimental testing of these isoxazoles as promising agents against HSP90 for the treatment of cancers shown in **Fig. 5**[86].

Natural Resources for Human Health
eISSN: 2583-1194

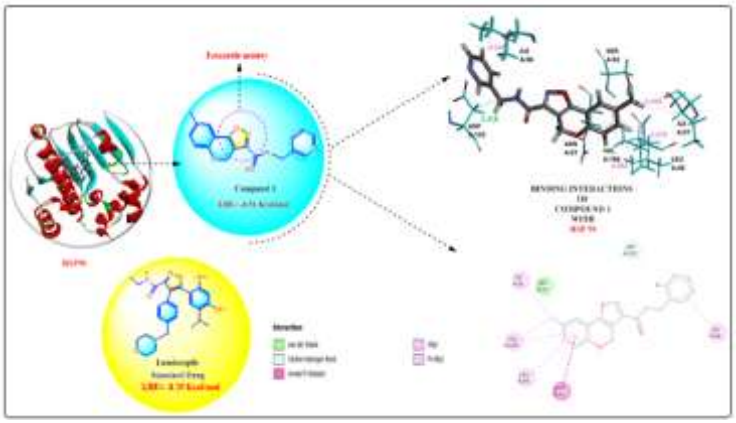


Fig. 5. Molecular docking study of potent compound 1 to HSP90 using Auto Dock showing docked complex, predicted docking score (LBE= -8.51 Kcal/mol), 3D representation shows interaction of ligand in grey colour with amino acids in green colour and 2D interaction profiles, along with comparison to standard inhibitor Luminespib.

Chandrasekaran *et al.*, 2025 Synthesized and evaluated a series of north heterocyclic substituted piperazine derivatives with Thieno[2,3-c] pyridine as the core because of their potential to fight cancer. These compounds were tested against different cancer cell lines such as breast cancer, head and neck cancer and colorectal cancer. The results showed that compounds 2 and 3 were the best inhibitors, with compound 3 showing broad activity against all cell lines tested. To understand the molecular level of action of these compounds, molecular docking studies were performed to investigate the molecular binding of these compounds to the HSP90 protein, which has been known to be a target in cancer treatment. These compounds interacted with significant amino acid residues such as Gly97, Asn51 and Lys58 through hydrogen bonds and hydrophobic contacts. Further, computational evaluations were carried out to check the drug-like properties and ADME characteristics of the synthesized compounds. Based on these findings, compound 3, which contains the thiomorpholine structure, was identified as a promising lead candidate to be further developed and optimized in anticancer treatments shown in **Fig. 6** [87].

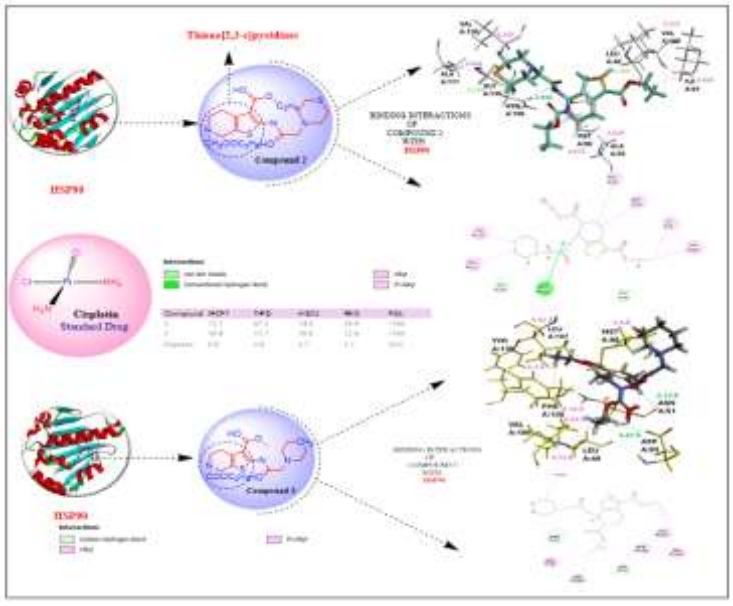


Fig. 6. A molecular docking investigation was carried out using Auto Dock to assess the interaction of compounds 2 and 3 with HSP90. Both compounds exhibited favourable predicted docking interactions, as supported by detailed 2D and 3D interaction analyses, and their performance was evaluated in comparison with the standard anticancer drug cisplatin. 3D representation of compound 2 shows interaction of the ligand in green colour with amino acids in grey colour, and 3D representation of compound 3 shows interaction of the ligand in grey colour with amino acids in yellow colour

Natural Resources for Human Health
eISSN: 2583-1194

Keshavarzipour *et al.,* 2024 designed, synthesized, and evaluated a new series of 3,4-di-substituted isoxazole compounds to see if they could inhibit heat shock protein 90 (HSP90), which plays a role in cancer progression. Using molecular docking studies, they found key interactions between the new compounds and specific amino acid residues within the HSP90 binding pocket, including Thr184, Asn51, Asp93, Asp58, Met98, and Val150. They also tested the cytotoxic effects of these compounds on MCF-7 and HeLa cancer cell lines as well as normal HUVEC cells by using an MTT assay. Compound 4 was especially effective and significantly reduced the HSP90 protein level from 5.54 ng/ml to 1.56 ng/ml in MCF-7 cells. Molecular dynamics simulations also showed that compound 4 was stably bound to the HSP90 active site. The study concluded that compound 4 and similar isoxazole derivatives are a promising class of HSP90 inhibitors with potential in the development of anti-cancer drugs shown in **Fig. 7** [88].

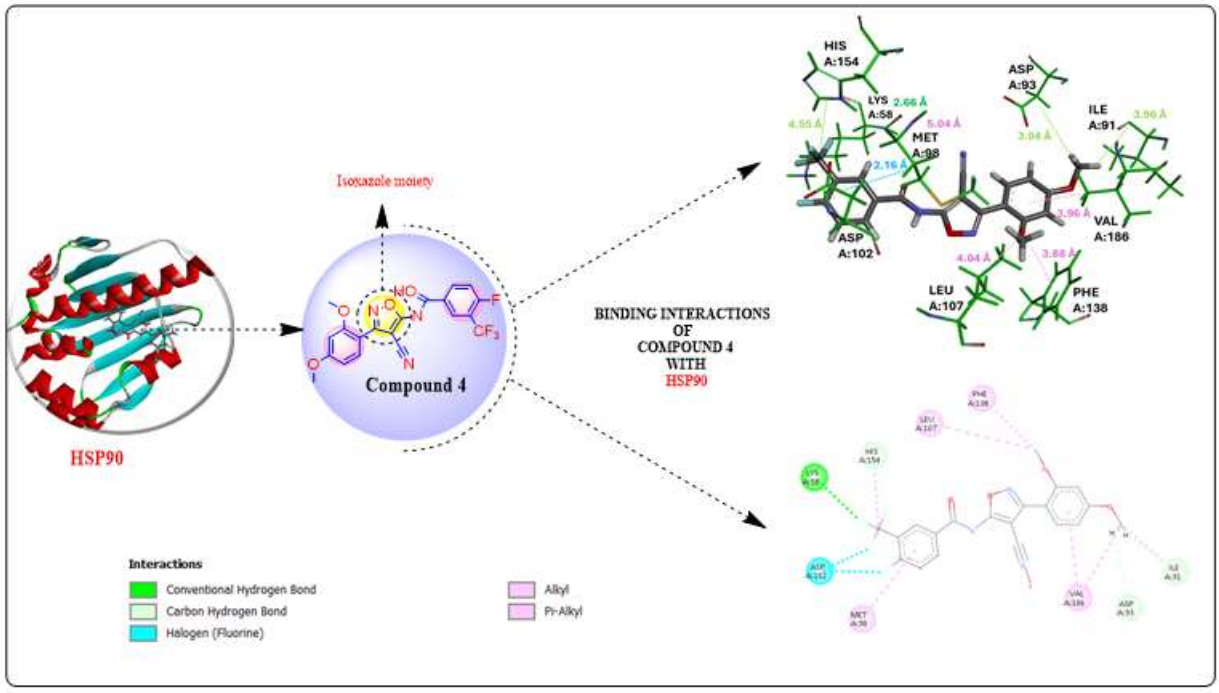


Fig. 7. Molecular docking study of potent compound 4 with HSP90 using Auto Dock, showing the docked complex along with a 3D representation showing the interaction of the ligand in grey colour with amino acids in green colour and 2D interaction profiles.

Xu et al., 2023: A structure-based virtual screening combined with molecular dynamics simulations was done to find new heat shock protein 90 (HSP90) inhibitors from an in-house database. Four compounds showed potential inhibitory activity against HSP90 ATPase, with compound HP-4 being the strongest. It had an IC50 of 17.64 ± 1.45 nM, which is about 7.7 times more potent than the known reference compound MPC-3100. Compound 5 interacts with important amino acid residues like Gly135, Asn106, Ala55, Leu107 and Asn51 through hydrogen bonds and hydrophobic contacts. Next, an in vitro cytotoxicity test showed that compound 5 significantly reduced the growth of several cancer cell lines, including HCT-116, HeLa, A549, A2780, DU145, HepG2, and A498. More importantly, in vivo studies using the HCT-116 xenograft model revealed that the growth of the tumor was greatly impeded by this compound. These results emphasized compound 5 as a lead compound that can be developed into specific HSP90 inhibitors in the treatment of cancer shown in **Fig. 8** [89].

Natural Resources for Human Health
eISSN: 2583-1194

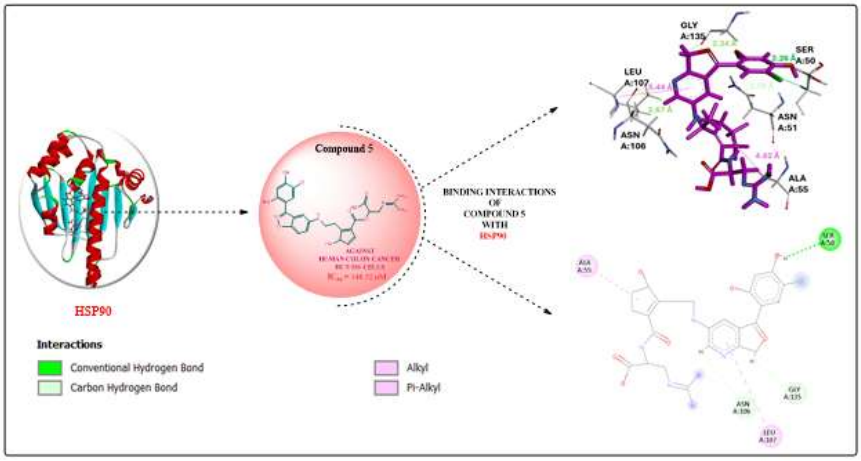


Fig. 8. Compound 5 was docked in the active site of HSP90 using Auto Dock to assess the cytotoxic activity. The compound showed very strong cytotoxic activity towards HCT116 cells with an IC50 value of 148.52 nM. The 2D interaction profile showed that there are crucial hydrogen bonding and hydrophobic contacts with active sites residues, whereas the 3D binding conformation showed stable accommodation of the ligand in the ATP-binding pocket of HSP90, hence suggesting its promising anticancer potential. 3D representations show the interaction of the ligand in pink with amino acids in grey.

Shin et al., 2020 synthesised and evaluated a targeted series of N7/N9-substituted purine compounds to assess their potential to inhibit heat shock protein 90 (HSP90). They explored how replacing the 4-methoxy-3,5-dimethylpyridine part of the known inhibitor BIIB 021 with simpler five-membered nitrogen- or oxygen-containing rings affected π-π stacking interactions within HSP90's hydrophobic pocket B and the shape of the outer α-helix 4. The inhibitory activity of the compounds against HSP90α was tested in cell-free assays. Several crystal structures were determined to gain insights into ligand binding. Notably, the isoxazole derivatives, along with the six-membered ring compound 6, showed high inhibitory activity. Compound 6 demonstrated promising anti-cancer activity against MCF-7, SK-BR-3, and HCT116 cell lines, and it interacted with important amino acid residues like Leu103, Leu107 and Phe138 through hydrogen bonds and hydrophobic contacts. Structural analysis indicated that the binding of these compounds stabilises the hydrophobic pocket and maintains the shape of the outer helix, which is critical for their biological activity, as shown in **Fig. 9** [41].

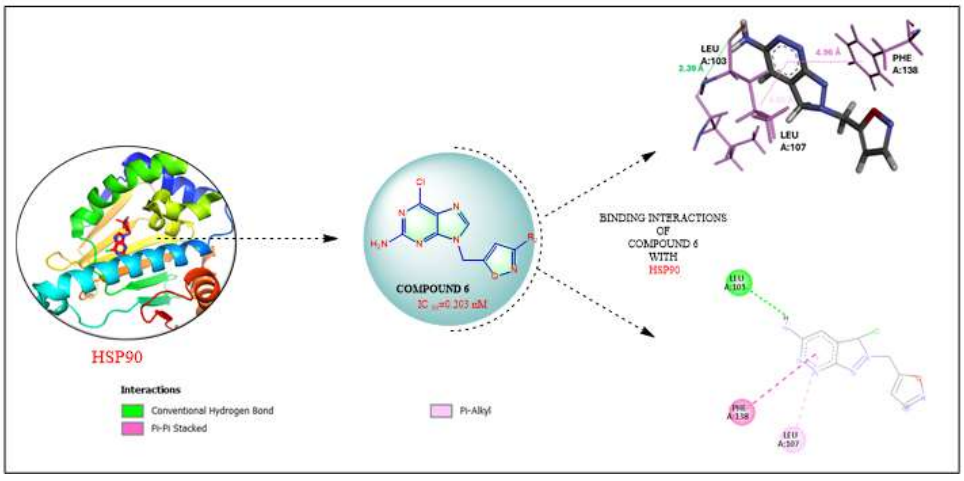


Fig. 9. Compound 6 was docked in the active site of HSP90 using Auto Dock to assess the docking analysis. The compound showed anti-cancer activity towards MCF-7, SK-BR-3, and HCT116 cell lines, with an IC50 value of 0.203 nM. The 2D interaction profile showed that there are crucial hydrogen bonding and hydrophobic contacts with active site residues, whereas the 3D binding conformation showed stable accommodation of the ligand in the ATP-binding pocket of HSP90, hence its promising anticancer potential. 3D representation shows the interaction of the ligand in grey with amino acids in pink.

Table 5: Computational methods facilitate compound prioritisation and identification of potential binding modes

Study	Computational approach	HSP90 target/site	Major computational findings	Experimental validation	Key limitation
Aboalroub et al. [86]	Structure-based similarity screening and molecular docking	N-terminal ATP-binding pocket	Identified compounds structurally related to Luminespib and predicted favourable interactions within the ATP-binding region	Experimental evaluation of selected compounds	Docking predictions alone cannot establish experimental affinity, selectivity, or clinical efficacy
Chandrasekaran et al. [87]	Molecular docking combined with synthesis and biological evaluation	HSP90 binding region	Docking was used to rationalise the interaction of piperazine-based derivatives with HSP90 and support structural optimisation	Cancer-cell cytotoxicity studies	Predicted ligand interactions require biochemical confirmation of direct HSP90 inhibition
Keshavarzipour et al. [88]	Molecular docking and molecular dynamics (MD) simulation	HSP90 ligand-binding region	Predicted stable interactions involving residues including Thr184, Asn51, Asp93, Met98 and Val150	Cytotoxicity assays and evaluation of HSP90 protein levels	MD stability does not directly demonstrate binding affinity or therapeutic efficacy
Xu et al. [89]	Virtual screening, molecular docking and MD simulation	N-terminal ATPase-binding site	Identified potential HSP90 inhibitors and examined the stability of protein–ligand complexes	Biochemical inhibition, cellular assays and HCT-116 xenograft study	Computational predictions remain dependent on protein preparation, scoring functions and simulation parameters
Shin et al. [41]	Structure-based ligand design, molecular docking and structural analysis	N-terminal HSP90α binding region	Explored the influence of N7/N9 substitutions on ligand recognition and interactions within the binding pocket	Cell-free HSP90α inhibition assays and experimentally determined crystal structures	Structural binding evidence is highly informative but does not alone establish clinical efficacy
Overall interpretation	Virtual screening + docking + MD + experimental validation	Mainly conserved N-terminal ATP-binding pocket	Computational methods facilitate compound prioritisation and identification of potential binding modes	Stronger evidence is obtained when computational predictions are supported by biochemical, structural and cellular data	Repeated targeting of the conserved ATP pocket may not adequately address isoform/paralog selectivity and clinical translation

Together, our findings show how computational techniques, such as evaluating complex stability, forecasting ligand-binding patterns, and ranking chemical candidates, can speed up the hunt for HSP90 inhibitors. However, rather than being direct indicators of experimental affinity or anticancer efficacy, docking scores and MD-derived stability should be regarded as computational evidence. The best research combines biochemical, structural, cellular, or in vivo confirmation with computer predictions. Crucially, most of the research on the conserved N-terminal ATP-binding region demonstrates that isoform or paralog selectivity is generally difficult to achieve. Therefore, protein conformational ensembles, nearby sub pockets, alternative or allosteric binding sites, and structural differences between HSP90 isoforms and paralogs that have been empirically verified should be considered in future computational studies.

5. CONCLUSION

HSP90 is an important therapeutic target in cancer because it is essential for maintaining the stability and functionality of many client proteins involved in tumor growth and survival. Structural studies have provided a comprehensive understanding of the domain organization, ATP-dependent chaperone cycle, and ligand-recognition properties of HSP90. Although the main structure of HSP90α and HSP90β is largely conserved, variations in sequence, residue numbering, local pocket environment, conformational behaviour, and biological function may present opportunities for the development of inhibitors. The investigation of HSP90–ligand structures indicate that residues such as Asp93, Lys58, Gly97, Phe138, and Thr184 contribute to ligand recognition inside or around the N-terminal ATP-binding domain Fig 10. However, interactions with conserved residues alone should not be interpreted as evidence of isoform selection. Similarly, individual docking scores should not be considered direct indicators of binding affinity or anticancer activity because they are computational estimates that must be confirmed by biochemistry and experiments.

The clinical development of HSP90 inhibitors has demonstrated that strong target binding and promising preclinical efficacy may not always transfer into outstanding clinical outcomes. Toxicity, adaptive heat-shock reactions, pharmacokinetic and pharmacodynamic limitations, insufficient therapeutic benefit, and problems achieving appropriate selectivity have all hindered clinical translation. These limitations imply that improving interactions within the highly conserved N-terminal ATP-binding region may not be sufficient to obtain a successful treatment window.

Therefore, future research on HSP90 inhibitors should consider adjacent subpockets, transient conformational states, structural features specific to isoforms or paralogs, C-terminal portions, and allosteric binding positions in addition to optimising the conserved ATP-binding pocket. By combining structural biology, molecular docking, molecular dynamics, biochemical testing, and experimental confirmation, promising binding hypotheses can be separated from interactions that do not produce biological activity. Pharmacokinetic properties, target engagement, tumor dependence on HSP90, and appropriate biomarkers should all be considered in lead optimisation. Such an integrated structure-guided strategy may help generate more selective and clinically efficacious HSP90 inhibitors with improved therapeutic characteristics.

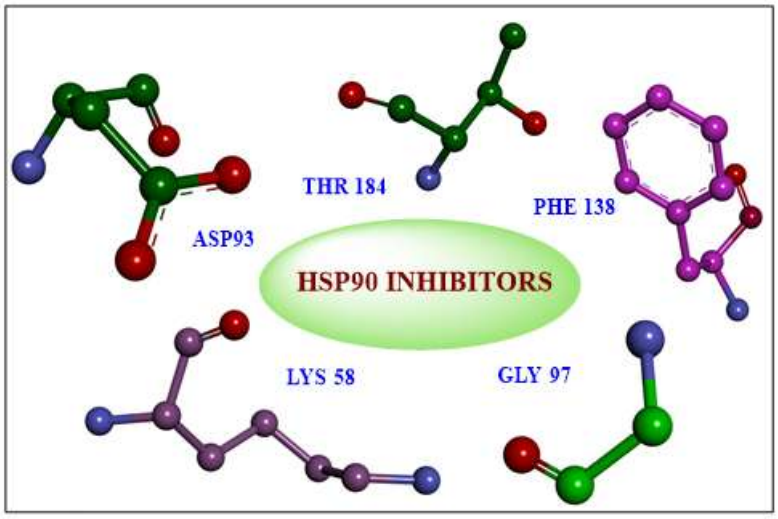


Fig. 10 Key HSP90 residues involved ligand recognition.

CONFLICT OF INTEREST

The authors declare that they have no conflict of interest.

ACKNOWLEDGMENT

The authors express their gratitude to the department of pharmaceutical chemistry, university institute of pharma science (UIPS) and UIPSR, Chandigarh University, Mohali-140413, Punjab, India for the support.

REFERENCES

[1] S. Kadavath, T. Conerly, A. Askell, T. Henighan, D. Drain, E. Perez, N. Schiefer, Z. H. Dodds, N. DasSarma, E. Tran-Johnson, *et al.*, "Language models (mostly) know what they know." 2022. Available: https://arxiv.org/abs/2207.05221

[2] S. C. Lin, J. Hilton, and O. Evans, "Teaching models to express their uncertainty in words," *Trans. Mach. Learn. Res.*, 2022. Available: https://arxiv.org/abs/2205.14334

[3] M. Xiong, Z. Hu, X. Lu, Y. Li, J. Fu, J. He, and B. Hooi, "Can LLMs express their uncertainty? An empirical evaluation of confidence elicitation in LLMs," in *Proceedings of the International Conference on Learning Representations*, 2024. Available: https://arxiv.org/abs/2306.13063

[4] Y. Ruan, H. Dong, A. Wang, S. Pitis, Y. Zhou, J. Ba, Y. Dubois, C. J. Maddison, and T. Hashimoto, "Identifying the risks of LM agents with an LM-Emulated sandbox," in *Proceedings of the International Conference on Learning Representations*, 2024. Available: https://arxiv.org/abs/2309.15817

[5] Z. Zhang, S. Cui, Y. Lu, J. Zhou, J. Yang, H. Wang, and M. Huang, "Agent-SafetyBench: Evaluating the safety of LLM agents." 2024. Available: https://arxiv.org/abs/2412.14470

[6] Q. Wu, G. Bansal, J. Zhang, Y. Wu, B. Li, E. Zhu, L. Jiang, X. Zhang, S. Zhang, J. Liu, *et al.*, "AutoGen: Enabling Next-Gen LLM applications via Multi-Agent conversation." 2023. Available: https://arxiv.org/abs/2308.08155

[7] S. Hong, M. Zhuge, J. Chen, X. Zheng, Y. Cheng, C. Zhang, J. Wang, Z. Wang, S. K. S. Yau, Z. Lin, *et al.*, "MetaGPT: Meta programming for a Multi-Agent collaborative framework." 2023. Available: https://arxiv.org/abs/2308.00352

[8] T. Guo, X. Chen, Y. Wang, R. Chang, S. Pei, N. V. Chawla, O. Wiest, and X. Zhang, "Large language model based Multi-Agents: A survey of progress and challenges." 2024. Available: https://arxiv.org/abs/2402.01680

[9] Y. Du, S. Li, A. Torralba, J. B. Tenenbaum, and I. Mordatch, "Improving factuality and reasoning in language models through multiagent debate," in *Proceedings of the International Conference on Machine Learning*, 2024. Available: https://arxiv.org/abs/2305.14325

[10] T. Liang, Z. He, W. Jiao, X. Wang, Y. Wang, R. Wang, Y. Yang, S. Shi, and Z. Tu, "Encouraging divergent thinking in large language models through Multi-Agent debate," in *Proceedings of the 2024 Conference on Empirical Methods in Natural Language Processing*, Association for Computational Linguistics, 2024, pp. 17889–17904. https://doi.org/10.18653/v1/2024.emnlp-main.992

[11] X. Wang, J. Wei, D. Schuurmans, Q. V. Le, E. H., S. Narang, A. Chowdhery, and D. Zhou, "Self-Consistency improves chain of thought reasoning in language models," in *Proceedings of the International Conference on Learning Representations*, 2023. Available: https://arxiv.org/abs/2203.11171

[12] M. K. Sivaraman, "The incident memory layer: An architectural component for lakehouse reliability," *Journal of Information Systems Engineering and Management*, vol. 9, no. 4, 2024.

[13] M. K. Sivaraman, "The reliability gap in modern lakehouse architectures: A failure fingerprinting framework for operational intelligence," *Current Journal of Applied Science and Technology*, vol. 45, no. 3, pp. 36–55, 2026. https://doi.org/10.9734/cjast/2026/v45i34673

[14] M. K. Sivaraman, "Closed-loop LLM-driven self-healing for enterprise data pipelines: Architecture and preliminary evaluation," in *Proceedings of the IEEE Technology and Innovation Conference (TIC)*, 2026.

[15] S. Yao, J. Zhao, D. Yu, N. Du, I. Shafran, K. Narasimhan, and Y. Cao, "ReAct: Synergizing reasoning and acting in language models," in *Proceedings of the International Conference on Learning Representations*, 2023. Available: https://arxiv.org/abs/2210.03629

[16] N. Shinn, F. Cassano, A. Gopinath, K. Narasimhan, and S. Yao, "Reflexion: Language agents with verbal reinforcement learning," in *Advances in Neural Information Processing Systems 36*, Neural Information Processing Systems Foundation, Inc. (NeurIPS), 2023, pp. 8634–8652. https://doi.org/10.52202/075280-0377

[17] G. Irving, P. F. Christiano, and D. Amodei, "AI safety via debate." 2018. Available: https://arxiv.org/abs/1805.00899

A. Smit, P. Duckworth, N. Grinsztajn, T. D. Barrett, and A. Pretorius, "Should we be going MAD? A look at Multi-Agent debate strategies for LLMs." 2023. Available: https://arxiv.org/abs/2311.17371

[18] M. Cemri, M. Z. Pan, S. Yang, L. A. Agrawal, B. Chopra, R. Tiwari, K. Keutzer, A. Parameswaran, D. Klein, K. Ramchandran, *et al.*, "Why do Multi-Agent LLM systems fail?" in *Advances in Neural Information Processing Systems 38*, Neural Information Processing Systems Foundation, Inc. (NeurIPS), 2025, pp. 135676–135729. https://doi.org/10.52202/085713-4082

[19] L. Yoffe, A. Amayuelas, and W. Y. Wang, "DebUnc: Improving large language model agent communication with uncertainty metrics," in *Findings of the Association for Computational Linguistics: EMNLP 2025*, Association for Computational Linguistics, 2025, pp. 23299–23315. https://doi.org/10.18653/v1/2025.findings-emnlp.1265

[20] B. Lakshminarayanan, A. Pritzel, and C. Blundell, "Simple and scalable predictive uncertainty estimation using deep ensembles." 2016. Available: https://arxiv.org/abs/1612.01474

[21] Y. Gal and Z. Ghahramani, "Dropout as a bayesian approximation: Representing model uncertainty in deep learning," in *Proceedings of the International Conference on Machine Learning*, 2016. Available: https://arxiv.org/abs/1506.02142

[22] C. Guo, G. Pleiss, Y. Sun, and K. Q. Weinberger, "On calibration of modern neural networks," in *Proceedings of the International Conference on Machine Learning*, 2017. Available: https://arxiv.org/abs/1706.04599

[23] L. Kuhn, Y. Gal, and S. Farquhar, "Semantic uncertainty: Linguistic invariances for uncertainty estimation in natural language generation," in *Proceedings of the International Conference on Learning Representations*, 2023. Available: https://arxiv.org/abs/2302.09664

[24] C. Chow, "On optimum recognition error and reject tradeoff," *IEEE Transactions on Information Theory*, vol. 16, no. 1, pp. 41–46, 1970. https://doi.org/10.1109/tit.1970.1054406

[25] R. El-Yaniv and Y. Wiener, "On the foundations of noise-free selective classification," *Journal of Machine Learning Research*, 2010.

[26] Y. Geifman and R. El-Yaniv, "Selective classification for deep neural networks." 2017. Available: https://arxiv.org/abs/1705.08500

[27] D. Hendrycks and K. Gimpel, "A baseline for detecting misclassified and Out-of-Distribution examples in neural networks," in *Proceedings of the International Conference on Learning Representations*, 2017. Available: https://arxiv.org/abs/1610.02136

[28] B. Wen, J. Yao, S. Feng, C. Xu, Y. Tsvetkov, B. Howe, and L. L. Wang, "Know your limits: A survey of abstention in large language models," *Transactions of the Association for Computational Linguistics*, vol. 13, pp. 529–556, 2025. https://doi.org/10.1162/tacl_a_00754

[29] Y. A. Yadkori, I. Kuzborskij, D. Stutz, A. György, A. Fisch, A. Doucet, I. Beloshapka, W.-H. Weng, Y.-Y. Yang, C. Szepesvári, *et al.*, "Mitigating LLM hallucinations via conformal abstention." 2024. Available: https://arxiv.org/abs/2405.01563

[30] S. Feng, W. Shi, Y. Wang, W. Ding, V. Balachandran, and Y. Tsvetkov, "Don't hallucinate, abstain: Identifying LLM knowledge gaps via Multi-LLM collaboration," in *Proceedings of the 62nd Annual Meeting of the Association for Computational Linguistics (Volume 1: Long Papers)*, Association for Computational Linguistics, 2024, pp. 14664–14690. https://doi.org/10.18653/v1/2024.acl-long.786

[31] D. Madras, T. Pitassi, and R. S. Zemel, "Predict responsibly: Improving fairness and accuracy by learning to defer," in *Proceedings of the Neural Information Processing Systems*, 2018. Available: https://arxiv.org/abs/1711.06664

[32] H. Mozannar and D. Sontag, "Consistent estimators for learning to defer to an expert." 2020. Available: https://arxiv.org/abs/2006.01862

[33] S. Amershi, D. Weld, M. Vorvoreanu, A. Fourney, B. Nushi, P. Collisson, J. Suh, S. Iqbal, P. N. Bennett, K. Inkpen, *et al.*, "Guidelines for Human-AI interaction," in *Proceedings of the 2019 CHI Conference on Human Factors in Computing Systems*, ACM, 2019, pp. 1–13. https://doi.org/10.1145/3290605.3300233

A. Z. Ren, A. Dixit, A. A. Bodrova, S. Singh, S. Tu, N. Brown, P. Xu, L. Takayama, F. Xia, J. Varley, *et al.*, "Robots that ask for help: Uncertainty alignment for large language model planners," in *Proceedings of the Conference on Robot Learning*, 2023. Available: https://arxiv.org/abs/2307.01928

[34] D. Amodei, C. Olah, J. Steinhardt, P. Christiano, J. Schulman, and D. Mané, "Concrete problems in AI safety." 2016. Available: https://arxiv.org/abs/1606.06565

[35] S. Naihin, D. Atkinson, M. Green, M. Hamadi, C. Swift, D. Schonholtz, A. T. Kalai, and D. Bau, "Testing language model agents safely in the wild." 2023. Available: https://arxiv.org/abs/2311.10538

[36] J. O. Kephart and D. M. Chess, "The vision of autonomic computing," *Computer*, vol. 36, no. 1, pp. 41–50, 2003. https://doi.org/10.1109/mc.2003.1160055

[37] P. Notaro, J. Cardoso, and M. Gerndt, "A survey of AIOps methods for failure management," *ACM Transactions on Intelligent Systems and Technology*, vol. 12, no. 6, pp. 1–45, 2021. https://doi.org/10.1145/3483424

[38] T. Ahmed, S. Ghosh, C. Bansal, T. Zimmermann, X. Zhang, and S. Rajmohan, "Recommending Root-Cause and mitigation steps for cloud incidents using large language models," in *2023 IEEE/ACM 45th International Conference on Software Engineering (ICSE)*, IEEE, 2023, pp. 1737–1749. https://doi.org/10.1109/icse48619.2023.00149

[39] Y. Chen, H. Xie, M. Ma, Y. Kang, X. Gao, L. Shi, Y. Cao, X. Gao, H. Fan, M. Wen, *et al.*, "Automatic root cause analysis via large language models for cloud incidents," in *Proceedings of the Nineteenth European Conference on Computer Systems*, ACM, 2024, pp. 674–688. https://doi.org/10.1145/3627703.3629553

[40] Z. Wang, Z. Liu, Y. Zhang, A. Zhong, J. Wang, F. Yin, L. Fan, L. Wu, and Q. Wen, "RCAgent: Cloud root cause analysis by autonomous agents with Tool-Augmented large language models," in *Proceedings of the 33rd ACM International Conference on Information and Knowledge Management*, ACM, 2024, pp. 4966–4974. https://doi.org/10.1145/3627673.3680016

[41] D. Roy, X. Zhang, R. Bhave, C. Bansal, P. Las-Casas, R. Fonseca, and S. Rajmohan, "Exploring LLM-Based agents for root cause analysis," in *Companion Proceedings of the 32nd ACM International Conference on the Foundations of Software Engineering*, ACM, 2024, pp. 208–219. https://doi.org/10.1145/3663529.3663841

[42] X. Zhou, G. Li, Z. Sun, Z. Liu, W. Chen, J. Wu, J. Liu, R. Feng, and G. Zeng, "D-Bot: Database diagnosis system using large language models," *Proceedings of the VLDB Endowment*, vol. 17, no. 10, pp. 2514–2527, 2024. https://doi.org/10.14778/3675034.3675043

[43] Y. Chen, M. Shetty, G. Somashekar, M.-J. Ma, Y. L. Simmhan, J. Mace, C. Bansal, R. Wang, and S. Rajmohan, "AIOpsLab: A holistic framework to evaluate AI agents for enabling autonomous clouds," *Conference on Machine Learning and Systems*, 2025. Available: https://arxiv.org/abs/2501.06706

[44] S. Jha, R. Arora, Y. Watanabe, T. Yanagawa, Y. Chen, J. Clark, B. Bhavya, M. Verma, H. Kumar, H. Kitahara, *et al.*, "ITBench: Evaluating AI agents across diverse Real-World IT automation tasks," in *Proceedings of the International Conference on Machine Learning*, 2025. Available: https://arxiv.org/abs/2502.05352

[45] M. Zaharia, A. Ghodsi, R. Xin, and M. Armbrust, "Lakehouse: A new generation of open platforms that unify data warehousing and advanced analytics," in *Conference on Innovative Data Systems Research*, 2021.

[46] M. Armbrust, T. Das, L. Sun, B. Yavuz, S. Zhu, M. Murthy, J. Torres, H. van Hovell, A. Ionescu, A. Łuszczak, *et al.*, "Delta lake: High-Performance ACID table storage over cloud object stores," *Proceedings of the VLDB Endowment*, vol. 13, no. 12, pp. 3411–3424, 2020. https://doi.org/10.14778/3415478.3415560

[47] S. Schelter, D. Lange, P. Schmidt, M. Celikel, F. Biessmann, and A. Grafberger, "Automating large-scale data quality verification," *Proceedings of the VLDB Endowment*, vol. 11, no. 12, pp. 1781–1794, 2018. https://doi.org/10.14778/3229863.3229867

[48] E. Breck, M. Zinkevich, N. Polyzotis, S. E. Whang, and S. Roy, "Data validation for machine learning," in *Proceedings of Machine Learning and Systems (MLSys)*, 2019, pp. 334–347. Available: https://openalex.org/W2946595616

[49] C. E. Shannon, "A mathematical theory of communication," *The Bell System Technical Journal*, vol. 27, no. 3, pp. 379–423, 1948. https://doi.org/10.1002/j.1538-7305.1948.tb01338.x

[50] K. Krippendorff, *Content analysis: An introduction to its methodology*. SAGE Publications, 2019. https://doi.org/10.4135/9781071878781

[51] Q. McNemar, "Note on the sampling error of the difference between correlated proportions or percentages," *Psychometrika*, vol. 12, no. 2, pp. 153–157, 1947. https://doi.org/10.1007/bf02295996

[52] E. R. DeLong, D. M. DeLong, and D. L. Clarke-Pearson, "Comparing the areas under two or more correlated receiver operating characteristic curves: A nonparametric approach," *Biometrics*, vol. 44, no. 3, p. 837, 1988. https://doi.org/10.2307/2531595

[53] S. Holm, "A simple sequentially rejective multiple test procedure," *Scandinavian Journal of Statistics*, 1979. https://doi.org/10.2307/4615733